Chemical Physics 123 (1988) 443–454
North-Holland, Amsterdam

THE DISSOCIATIVE ELECTROIONIZATION OF AMMONIA AND AMMONIA-d_3. I. THE NH^+ AND NH_2^+ DISSOCIATION CHANNELS

R. LOCHT, Ch. SERVAIS, M. LIGOT, Fr. DERWA and J. MOMIGNY
Département de Chimie Générale et de Chimie Physique, Institut de Chimie, Bâtiment B6, Université de Liège, Sart-Tilman par B-4000 Liège 1, Belgium

Received 25 February 1988

The dissociative electroionization of NH_3 (ND_3), in the NH_2^+ (ND_2^+) dissociation channels, is investigated in the 15–50 eV electron energy range. The translational energy distributions of ND_2^+ (NH_2^+) exhibit several components, whereas NH^+ only shows a continuous, broad distribution. For both ions a kinetic energy versus appearance energy diagram is obtained and discussed. The predissociation of the Jahn–Teller split $NH_3^+(\tilde{A}\,^2E)$ state produces both ions at their lowest threshold. At higher energies, dissociative autoionization (in the 22 eV region), dissociative ionization through the $NH_3^+(\tilde{B}\,^2A_1)$ state in (the 24–30 eV region) as well as dissociation by Coulomb repulsion of doubly ionized states (in the 35–50 eV region) produce NH_2^+ (ND_2^+) and NH^+ with large amounts of translational energy. Some arguments are brought forward to indicate that the former value of the NH_2–H dissociation energy is overestimated.

1. Introduction

Owing to its major importance in many fields, the ionization of ammonia has been investigated in detail by almost all experimental techniques available today. Comparatively, the study of the dissociative ionization of this molecule has scarcely been touched on.

Though it has been studied by dissociative electroionization [1–4], photoionization [5,6], charge transfer [7], photoion–photoelectron coincidence spectroscopy [8] and by quantum mechanical calculations [9], the NH_2^+ dissociation channel has mainly been studied in the lowest onset-energy region. Only thermal and nearly thermal translational energies are considered. Recently evidence has been brought to its formation through the decomposition of the first doubly ionized state of NH_3 [10]. Even fewer data are available on the dissociation of NH_3 into NH^+. Onset energies of this ion were measured by electron impact and charge transfer [1–4,7]. These results were barely discussed. No kinetic energy data are available. Branching ratios for dissociation of NH_3 through its three ionic states were obtained by electron–ion coincidence and dipole (e,2e) electron impact coincidence methods [11,12].

The aim of this work is to investigate in detail all dissociation channels of NH_3 by using the electroionization mass spectrometry method including ion translational energy analysis. The electron energy of 12–100 eV has been covered, enabling us to extend this work to the study of doubly ionized species, i.e. NH_3^{2+} and N^{2+}. Preliminary results on this particular aspect have been reported elsewhere [13].

In the present paper the results on NH_2^+ and NH^+ are presented and discussed. A comparative study of the corresponding ions in ND_3 is included when necessary.

2. Experimental

The experimental setup used in the present study has been described in detail earlier [14]. Only the prominent features and the most important modifications will be mentioned here.

The ions produced in a Nier-type ion source by the impact of energy-controlled electrons are allowed to drift out of the ion chamber, are focused on the ion source exit hole, energy-analysed with a retarding lens and mass-selected in a quadrupole mass filter. The ion current, collected on a 17-stage Cu–Be electron

0301-0104/88/$ 03.50

multiplier, is continuously scanned as a function of either the electron energy at fixed retarding potential V_R or the retarding potential at fixed electron energy E_e. Both signals are electronically differentiated.

The most important variable parameters of the experiment, i.e. the electron energy, the retarding potential, the multiplier high voltage as well as the mass m/e setting are presently computer-controlled [15]. The computer is programmed for a preset number of scans under preset experimental conditions. A sequence of up to 16 experiments could be programmed. The averaged curves are sent to a minicomputer to be stored for further handling and recording.

The ammonia, of 99.95% purity, purchased from Air Liquide, was carefully desiccated and distilled under vacuum. The ammonia-d_3, purchased from Merck, Sharp & Dohme, of 99.7 at% purity, has been handled in the same way. The purity of the samples was checked by mass spectrometry.

Special attention has been payed to keep the background mass spectrum as low as possible. The major contaminant is H_2O. Therefore prolongated bake-out of the vacuum chamber has been practiced until a residual gas pressure of about 2×10^{-8} Torr was reached. The sample is introduced at a pressure of 10^{-7} Torr in the vacuum vessel.

The maximum of the NH_3^+ ion energy distribution is used as the zero-energy calibration point for the translational energy scale. The same reference is used during the recording of the ionization efficiency curves of the fragment ions at different retarding potential settings.

For the electron energy scale calibration, the first ionization energy of Ar (15.759 eV) [16] and Ne (21.564 eV) [16] was used for NH_2^+ (ND_2^+) ions. The good reproducibility (less than 0.1 eV) of the first appearance energy of NH_2^+ allowed us to choose this energy as an internal standard for the appearance energy measurements of all the other investigated fragment ions. The linear extrapolation method used to determine the threshold energy has fully been described previously [14].

For each fragment ion, at each retarding potential or electron energy setting, the first derivative of the ionization efficiency or of the retarding potential curve is scanned 100–800 times, depending on the ion intensity. This procedure is repeated at least five times. The energies reported in the next sections are averaged values of these independent measurements. The quoted errors and drawn error bars represent the standard deviation. In the kinetic energy versus appearance energy diagrams, linear regressions are fitted to the experimental data.

3. Experimental results

3.1. The NH_2^+ dissociation channel

The measurements on this dissociation channel were made by using ND_3. The reasons for this choice will clearly appear below.

The kinetic energy distribution of ND_2^+, as given by the first derivative of the retarding potential curves, is shown in fig. 1 for different electron energies E_e. This distribution shows three components in the 100–50 eV electron energy range: (i) a very intense peak with a maximum at thermal energy, (ii) a shoulder at 0.37 ± 0.01 eV and (iii) a well-resolved peak with a maximum at 0.65 ± 0.03 eV. The shoulder at 0.37 eV disappears between 45 and 30 eV electron energy. The intensity ratios of these three contributions are about 100:2:1 respectively.

Interference between ND_2^+ and H_2O^+ might be suspected at $m/e=18$. The intensity ratio of the background signal H_2O^+ over the ND_2^+ ion was less than 1% at 75 eV electron energy. However, for higher retarding potential settings (>0.2 V), the H_2O^+ parent ion is suppressed and the weak high-energy contributions at 0.37 and 0.65 eV can unambiguously be ascribed to ND_2^+. A similar but less favorable situation is observed at $m/e=16$ where both the fragments NH_2^+/NH_3 and O^+/H_2O and O_2 could be observed. At high ion energies, even impurities of very low intensity could have relatively appreciable contributions.

A typical first differentiated ionization efficiency curve of ND_2^+, as observed with a slightly negative retarding potential setting and in the electron energy range 14–50 eV, is shown in fig. 2. Six threshold energies, five of which are indicated by a vertical bar, are measured over this range, i.e. 15.72 ± 0.04, 21.3 ± 0.3, 22.6 ± 0.3, 35.4 ± 0.2, 37.6 ± 0.2 and 46.5 ± 0.4 eV. For NH_2^+/NH_3 the first onset is measured at

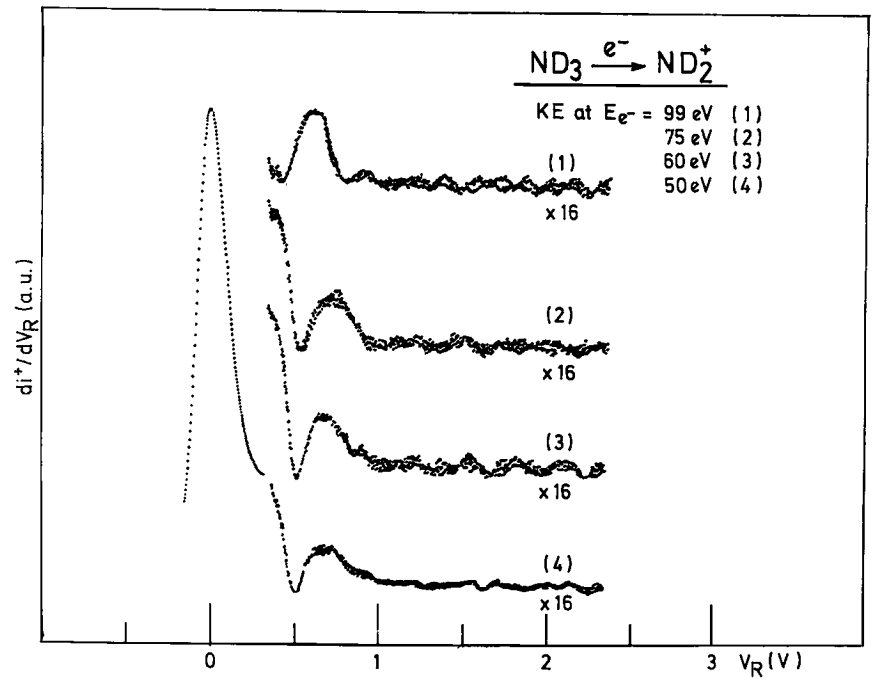

Fig. 1. The kinetic energy distribution curves of ND_2^+/ND_3 as observed at indicated electron energies.

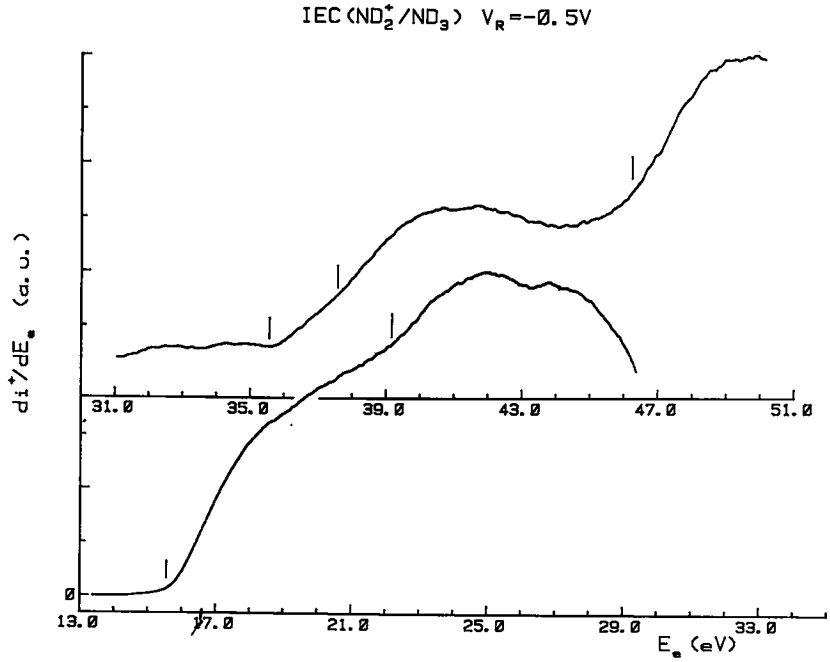

Fig. 2. The first differentiated ionization efficiency curve ND_2^+/ND_3 from the onset up to 50 eV, as observed at $V_R = -0.5$ V. Vertical bars locate the average appearance energies.

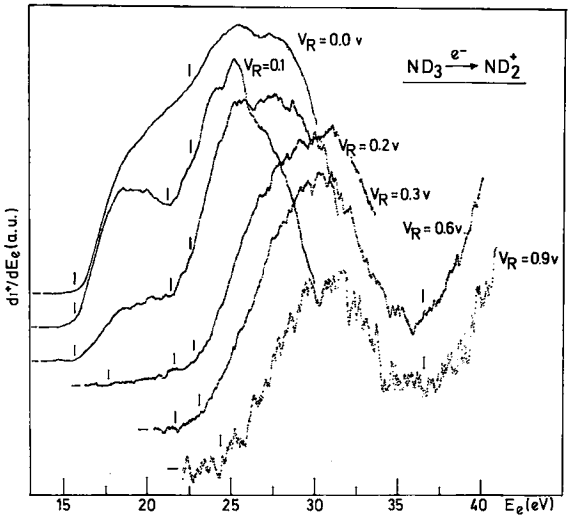

Fig. 3. A typical set of first differentiated ionization efficiency curves of ND_2^+/ND_3 as observed at indicated V_R settings. Vertical bars located the average appearance energies.

15.76 ± 0.05 eV. The first differentiated ionization efficiency curve of ND_2^+ has been recorded at intervals of 0.1 V between 0 and 0.9 V retarding potential (see fig. 3). Drastic changes of the shape of these curves have to be noticed, e.g., the first steeply rising portion is suppressed within 0.2 V retarding potential. The results of the measurements of the appearance energies (AE) at each retarding potential setting V_R are displayed in the diagram shown in fig. 4.

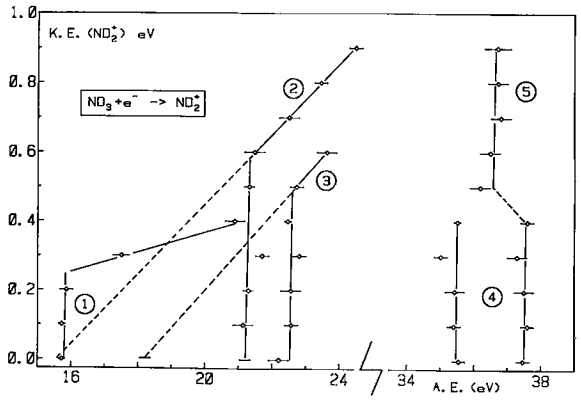

Fig. 4. The kinetic energy (KE) versus appearance energy (AE) plot for ND_2^+/ND_3.

3.2. The NH^+ dissociation channel

The translational energy distribution of NH^+, as obtained by the first differentiated retarding potential curve, has been recorded between 18 and 100 eV electron energy. Fig. 5 displays a set of translational energy distributions near the onset of NH^+, i.e. for 18–30 eV electrons.

This distribution is essentially continuous. However, considering the fraction (2/17) of the total translational energy carried by the ion, it appears unusually broad and it shows a tail extending up to 1.4 eV for 100 eV electrons. Thermally distributed NH^+ ions are only observed close to the lowest onset. For increasing electron energies, the distribution is regularly broadened and its maximum shifts toward high ion energies, as shown in fig. 6. This unusual behaviour would at least indicate that only the NH^+ ions, produced at the lowest onset, are thermal and of low intensity. A few eV above this threshold the maximum shifts significantly, meaning that only energetic NH^+ ions are formed.

A typical first differentiated ionization efficiency curve of NH^+, recorded with a slight negative retard-

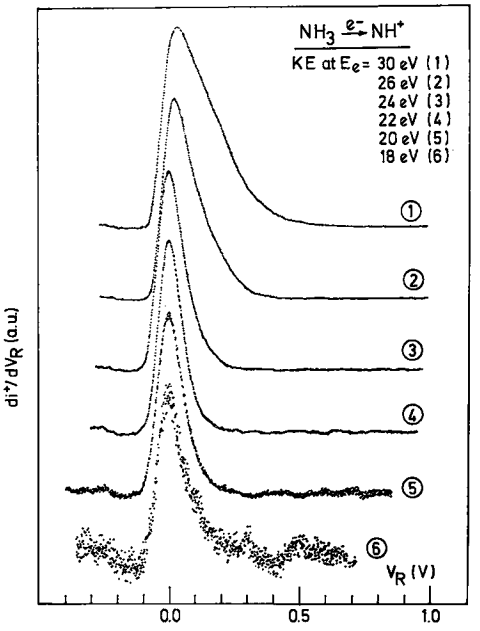

Fig. 5. The kinetic energy distribution curves of NH^+/NH_3 as observed between 18 and 30 eV electron energy.

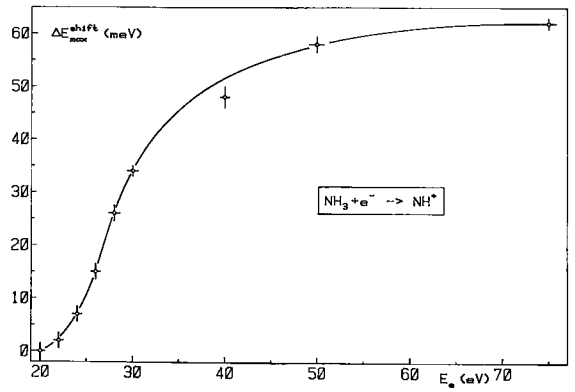

Fig. 6. Electron energy dependence of the maximum of the NH^+ kinetic energy distribution. For explanation see text.

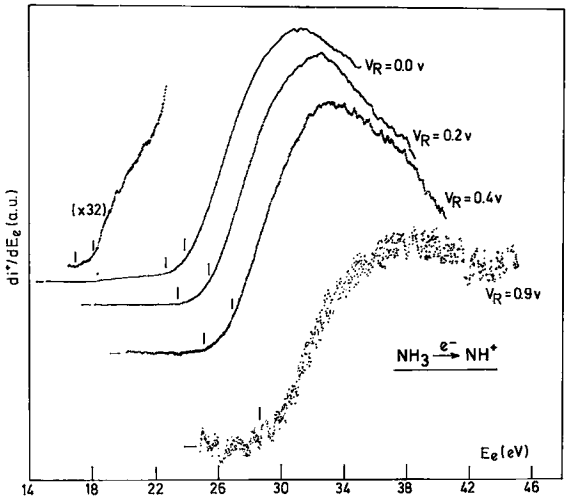

Fig. 8. A typical set of first differentiated ionization efficiency curves of NH^+/NH_3 as observed for indicated V_R settings. Vertical bars locate the average appearance energies.

ing potential between 12 and 50 eV electron energy, is shown in fig. 7.

Six onset energies are measured in this energy range, i.e. 16.9 ± 0.1, 18.0 ± 0.2, 22.6 ± 0.2, 24.4 ± 0.3, 36.2 ± 0.3 and 46.4 ± 0.5 eV. The low-energy side of the first differentiated ionization efficiency curve of NH^+ has been recorded by steps of (i) 0.05 V between 0 and 0.2 V and (ii) 0.1 V between 0.2 and 1.0 V retarding potential. A typical set of curves is displayed in fig. 8. As already pointed out for ND_2^+, the first two steeply

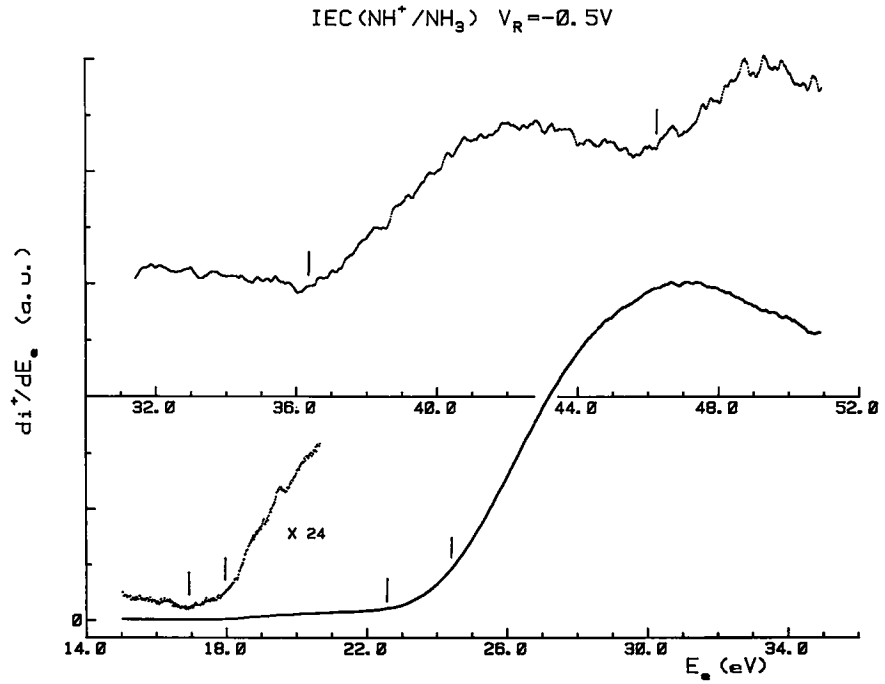

Fig. 7. The first differentiated ionization efficiency curve of NH^+/NH_3 from the onset up to 50 eV as observed at $V_R = -0.5$ V. Vertical bars locate the average appearance energies.

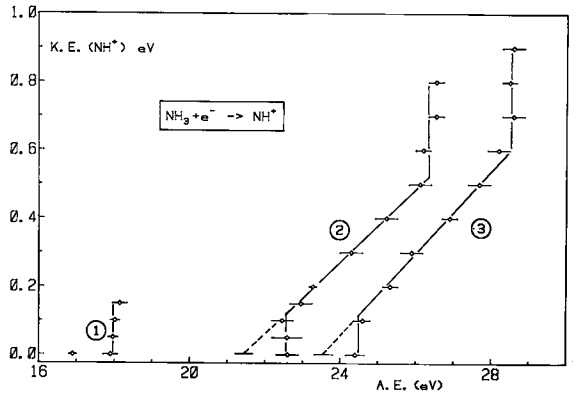

Fig. 9. The kinetic energy (KE) versus appearance energy (AE) plot for NH^+/NH_3.

rising portions, of low intensity, are suppressed within 0.15 V retarding potential. This ion current only will contribute to the thermal peak observed in the ion kinetic energy distribution. Fig. 9 shows the diagram obtained by plotting the appearance energies (AE) measured for each retarding potential V_R. For the high-energy processes, with onsets observed at 36.2 and 46.4 eV, the same plot is shown in fig. 10.

4. Discussion

For the easiness and clarity in the following discussions, all data used to calculate the threshold energies for dissociative ionization processes giving rise to NH_2^+ and NH^+ from NH_3, are collected in table 1.

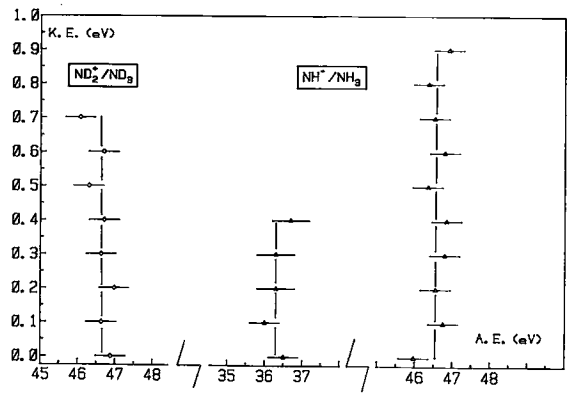

Fig. 10. The kinetic energy (KE) versus appearance energy (AE) plot for ND_2^+/ND_3 and NH^+/NH_3 in the energy range around 45 eV and 36–48 eV respectively.

Table 1
Dissociation (D), ionization (IE) and excitation (EE) energies (eV) of NH_3, NH_2, NH, H_2 and H used in this work [a]

$D(NH_2\text{–}H)=4.51\pm0.09$ [b]	$EE(NH_2^+(\tilde{X}\,^3B_1))=0.0$
$D(NH\text{–}H)=3.90\pm0.09$ [b]	$EE(NH_2^+(\tilde{a}\,^1A_1))=0.99$ [e]
$D(H_2)=4.476$ [c]	$EE(NH_2^+(\tilde{b}\,^1B_1))=2.23$
$IE(H)=13.598$ [d]	$EE(NH^+(X\,^2\Pi))=0.0$
$IE(NH_2)_{ad.}=11.46\pm0.01$ [c]	$EE(NH^+(a\,^4\Sigma^-))=0.044$ [f]
$IE(NH_2)_{vert.}=12.0$	$EE(NH^+(A\,^2\Sigma^-))=2.674$
$IE(NH)_{ad.}=13.49\pm0.01$ [c]	$EE(NH^+(B\,^2\Delta))=2.847$
	$EE(NH^+(C\,^2\Sigma^+))=4.409$

[a] 1 eV = 23.060 kcal mol^{-1} = 8 065.73 cm^{-1}.
[b] Ref. [17]. [c] Ref. [18]. [d] Ref. [16]. [e] Ref. [19].
[f] Ref. [20].

The results obtained in this work for these ions, are summarized in table 2.

The NH_3 molecule, belonging to the C_{3v} symmetry group, has a ground state configuration given by

$$(1a_1)^2(2a_1)^2(1e)^4(3a_1)^2\ \tilde{X}\,^1A_1\ .$$

Three ionic states are observed by HeI [21] and HeII [22,23] photoelectron spectroscopy: the $\tilde{X}\,^2A_1$ $(3a_1^{-1})$ at 10.073 eV, the $\tilde{A}\,^2E$ $(1e^{-1})$ at 14.725 eV and the $\tilde{B}\,^2A_1$ $(2a_1^{-1})$ at about 24 eV. Though the ground state shows an extended, well-resolved vibrational structure, the first excited state, spread over about 4 eV, exhibits a more diffuse vibrational structure and underlying continua. The third valence band, essentially structureless, extends from about 24 to 30 eV. The 30–70 eV energy range, investigated by Au-

Table 2
The kinetic energy distributions (KED) and appearance energies (AE) (eV) measured in this work for ND_2^+ (NH_2^+) and NH^+

	KED	AE
ND_2^+ (NH_2^+)	0.00	15.72 ± 0.04
	(0.37 ± 0.01)	22.6 ± 0.1
	(0.65 ± 0.03)	21.3 ± 0.3
		35.4 ± 0.3
		$37.6/36.6\pm0.3$
		46.5 ± 0.4
NH^+	continuous,	16.9 ± 0.1
	shifting max.	18.0 ± 0.2
		22.6 ± 0.3
		24.4 ± 0.3
		36.2 ± 0.4
		46.4 ± 0.5

ger electron spectroscopy, corresponds to the double ionization of NH_3 [24,25].

4.1. The NH_2^+ dissociation channel

Except when otherwise stated, no distinction will be made between NH_2^+ and ND_2^+.

The first onset observed for NH_2^+ and ND_2^+ lies respectively at 15.76 ± 0.05 and 15.72 ± 0.04 eV as measured with respect to Ne and Ar. This value agrees with previous determinations by electroionization [1,2] and photoionization [5].

The kinetic energy versus appearance energy diagram related to this process is the vertical line (1) in fig. 4, followed by a quasi-horizontal line corresponding to a "jump" of 5.6 eV electron energy for a kinetic energy difference of 0.1 eV. This sudden breakup in the diagram correlates with the electronic excitation of the molecular ion and/or the fragment ion. On the other hand, the invariability of the appearance energy with the kinetic energy carried by the fragment ion could mainly be interpreted in two ways: (i) the fragmentation process proceeds through a mechanism where the total excess energy is partitioned between translational and internal energy and (ii) a scan through the thermal distribution. In the former case, the vertical line usually covers several tenth to several eV kinetic energy, in the latter the vertical line is spread over 0.2–0.3 eV, i.e. the half full width of the thermal distribution. This is observed for ND_2^+ and consequently the fragment ion is produced without translational energy. The steepness of the ionization efficiency curve at the onset, as well as the narrowness of the kinetic energy range tend to support this interpretation.

The lowest threshold calculated from the data of table 1 for the appearance of NH_2^+ through

$$NH_3 + e^- \rightarrow NH_2^+ (\tilde{X}\,^3B_1) + H\,(^2S_g) + 2e^-$$

lies at 15.97 ± 0.1 eV. This value is in excess by about 0.2 eV, even with the photoionization value, i.e. 15.73 ± 0.02 eV [5] or 15.768 ± 0.004 eV [6] which is the extrapolated onset to 0 K. From the former value and the adiabatic ionization energy of NH_2 [19], a dissociation energy $D\,(NH_2\text{–}H) = 4.27 \pm 0.03$ eV is deduced.

Contrarily, in the first interpretation, the total excess energy to be partitioned between translational and internal energy would be at least $0.2 \times 20/2 = 2$ eV for ND_2^+. This value, included in the energy balance, would lower the $D(NH_2\text{–}H)$ value by the corresponding quantity.

As pointed out by many authors [2,6,8,11,12,21], the appearance energy of ND_2^+ (NH_2^+) lies 1 eV above the adiabatic ionization energy of the $\tilde{A}\,^2E$ electronic excited state of NH_3^+. However, the dissociation products correlate with the NH_3^+ ($\tilde{X}\,^2A_1$) state in the C_{3v} symmetry group [9]. The ^2E state exhibits discontinuous and irregular vibrational structure perhaps superposed on continua [21]. An apparent interrupt in the vibrational structure is observed between 15.9 and 16.25 eV, i.e. the energy range where ND_2^+ (NH_2^+) ions are produced. Several authors [8,21] showed Jahn–Teller forces being operative in the ^2E state. Krier et al. [9] made a quantum mechanical description of the link, a conical intersection, between the $\tilde{X}\,^2A''$ and the $\tilde{A}\,^2A''$ Jahn–Teller component of the ^2E state in C_s point group. This link allows the NH_3^+ (^2E) species to find the dissociation path through predissociation by radiationless transition to the dissociation continuum of the NH_3^+ ($\tilde{X}\,^2A_1$).

The second onset, only measured for ND_2^+, is observed at 22.6 eV (see fig. 3). However, for higher retarding potential settings, two onsets are observed, i.e. at 21.3 ± 0.3 and 22.6 ± 0.1 eV. The kinetic energy versus appearance energy diagrams related to this energy are labeled by (2) and (3) in fig. 4.

At 21.2 ± 0.3 eV a vertical line followed by a straight line is observed. A least-squares fit of the experimental data yields a slope of 0.1 and extrapolates to 15.5 eV with a correlation coefficient of 0.999. The slope has to be compared with the ratio $m_D/m_{ND_3} = 2/20 = 0.1$. The straight line spreads from 0.6 to 0.9 eV translational energy. These ND_2^+ ions contribute to the 0.65 eV peak observed in the translational energy distribution. The minimum kinetic energy carried by ND_2^+ in this process has to be about 0.6 eV. The agreement between experimental and expected slopes indicates total conversion of the excess energy into translational energy.

The energy of 21.2 eV lies between the $\tilde{A}\,^2E$ and $\tilde{B}\,^2A_1$ states of NH_3 where no direct ionization cross section is measured for NH_3. Dissociative autoionization would produce ND_2^+ at this energy through

$$ND_3 + e^- \longrightarrow ND_3^{**} + e^- \text{ (autoion. to } 3a_1 \text{ contin.)}$$
$$\hookrightarrow ND_2^+(\tilde{X}\,^3B_1) + D(^2S_g) + KE_{min}(6\,eV) + e^- .$$

At 22.6 eV (see diagram 3 in fig. 4) a straight line with a slope of 0.1 is drawn through the experimental data defined by only two measurements. It extrapolates to about 18 eV. A minimum translational energy of 0.5 eV is carried by ND_2^+ ions which are the second contribution to the 0.65 eV peak (see fig. 1). The energy difference between the two extrapolated values, i.e. $18-15.5=2.5$ eV, can be compared with the excitation energy of ND_2^+ in its $\tilde{B}\,^1B_1$ state. By photoelectron spectroscopy the $\tilde{X}\,^3B_1$–$\tilde{B}\,^1B_1$ energy gap for ND_2^+ is 2.23 ± 0.02 eV (see table 1) [19]. As for the process at 21.3 eV, the ND_2^+ ions with their onset at 22.6 eV have to be produced through a dissociative autoionization mechanism

$$ND_3 + e^- \longrightarrow ND_3^{**} + e^- \text{ (autoion. to 1e contin.)}$$
$$\hookrightarrow ND_2^+(\tilde{b}\,^1B_1) + D(^2S_g) + KE_{min}(5\,eV) + e^- .$$

Morrison and Traeger [2] detected fine structures in their first differentiated electroionization efficiency curves. These authors ascribed these features to autoionization. Both Wight et al. [11] and Brion et al. [12] mentioned an "interesting feature extending from 25 to 35 eV [11] (or 22–34 eV [12]) in the partial oscillator strength. This "bump" would arise from the excitation of Rydberg states associated with the $2a_1$ ionization limit and autoionizing to the $3a_1$ ionic state".

The two dissociative autoionization processes just discussed would be a further evidence of the existence of these Rydberg states. As will be seen below (for NH^+) and in a future publication, these Rydberg states play an important role in all dissociation channels of NH_3 leading to NH^+, N^+, H_2^+ and H^+.

In the present work, no evidence is found for ND_2^+ formation through the decomposition of the ND_3^+ ($\tilde{B}\,^2A_1$) upper valence state at 24 eV, as suggested earlier by Morrison and Traeger [2].

Above the valence electron ionization energy range, three onsets are measured, i.e. 35.4 ± 0.3, 37.6 ± 60.3 and 46.5 ± 0.4 eV. The corresponding kinetic energy versus appearance energy diagrams are shown in fig. 4, labeled (4) and (5). The 46.5 eV onset, represented in fig. 10, is observed for $0.0 < V_R < 0.7$ V. The shoulder observed in the kinetic energy distribution at 0.37 V (see fig. 1) has an "onset" between 40 and 30 eV.

In the electron energy range above 34 eV, doubly ionized states of NH_3 are detected [10,13,24]. These states dissociate by Coulomb repulsion giving rise to fragments carrying large amounts of kinetic energy. Obviously the two separating ionized fragments are characterized by the same appearance energy. In spite of their instability, doubly ionized states are usually characterized by a shallow minimum for short internuclear distances. A potential barrier separates the "stable" part from the repulsive region of the hypersurface.

The first vertical line (4) at 35.4 ± 0.3 eV extends to 0.4–0.5 eV translational energy carried by ND_2^+, i.e. 4–5 eV in terms of total kinetic energy. For both H^+ and D^+ a probably related onset has been measured at 34.9 ± 0.4 eV [26]. Consequently a dissociation limit, leading to the production of both ions, would lie at 31.4–30.4 eV. The lowest threshold calculated for the dissociation of ND_3 into ND_2^+ and D^+ by

$$ND_3 + e^- \longrightarrow ND_3^{2+}(^3E(1e^{-1}, 3a_1^{-1})) + 3e^-$$
$$\hookrightarrow ND_2^+(\tilde{X}\,^3B_1) + D^+(^1S_g)$$

is at 29.53 ± 0.1 eV (from the data of table 1). This value is at least about 1 eV lower than the predicted energy 31.4–30.4 eV. In the C_{3v} symmetry group, the dissociation products correlate with a $NH_3^{2+}(^3E)$ state. The ionization energy of this state has been calculated at 37.3 eV for a $(1e^{-1}, 3a_1^{-1})$ configuration [25]. This energy is too high to be related with the ND_2^+ onset measured at 35.4 ± 0.3 eV. However, a lower-lying $ND_3^{2+}(^1A_1)$ state has been calculated at 35.6 eV [25] and observed at 35.4 eV [10], 34.9 eV [13], and 33.1 eV [24]. The symmetry of this state in the C_{3v} point group is compatible with the dissociation process

$$ND_3 + e^- \longrightarrow ND_3^{2+}(^1A_1, (3a_1^{-2})) + 3e^-$$
$$\hookrightarrow ND_2^+(^1A_1) + D^+(^1S_g) ,$$

for which an onset energy is calculated at 30.5 eV (see table 1) and in better agreement with the predicted dissociation level of 31.4–30.4 eV. The same dissociation mechanism of NH_3^{2+} has been observed by photoion–photoion coincidence technique at a photon energy of 35.4±0.5 eV [10]. Furthermore the closeness of the ionization potential of 34.9±0.2 eV [13] and the appearance energy of the fragments, i.e. 35.4±0.3 eV for ND_2^+ and 34.9±0.4 eV for D^+ [26], as measured with the same instrument, would be indicative of a low potential barrier. The absence of a straight line with a slope would mean that the vertical transition takes place at or close to the level of the upper edge of the barrier.

The "broken" vertical line (5) in fig. 4 shows a branch at 37.6±0.3 eV and at 36.6±0.3 eV. Probably the onset 36.6 eV is shifted to higher energies by the lower-lying contribution. At this onset the ND_2^+ ion carries 0.8–0.9 eV kinetic energy, i.e. 8–9 eV total translational energy. An onset is observed for H^+ and D^+ at 36.2±0.3 eV [26]. As pointed out earlier, ND_2^+ and D^+ showing about the same onset could be considered as being produced by the dissociation of the same ND_3^{2+} state. However, it has to be kept in mind that at the same energy NH_2^+ (ND_2^+) could simultaneously be formed with other products, i.e. H and/or H* [27,28]. The dissociation limit of the state involved would be at 28.6–27.6 eV, which could be compared to the energy of 29.5 eV calculated for

$$ND_3 + e^- \longrightarrow ND_3^{2+}(^3E(1e^{-1}, 3a_1^{-1})) + 3e^- \hookrightarrow ND_2^+(\tilde{X}\,^3B_1) + D^+(^1S_g),$$

where the $ND_3^{2+}(^3E)$ state has a calculated ionization energy of 37.3 eV [25], close to the appearance energy determined for ND_2^+.

The third threshold in the high-energy range lies at 46.5±0.4 eV and the kinetic energy carried by ND_2^+ is estimated to be 0.7 V. Consequently the dissociation limit would be at about 39.5 eV. The only appearance energy measured for D^+ in the corresponding energy range is at 46.1±0.5 eV [26]. Apparently, both onsets are correlated. However, several ions, e.g. NH^+ and N^+, show a threshold at the same energy. Furthermore, the production of singly ionized fragments with neutrals could not be ruled out. Neutral species, i.e. high Rydberg H atoms [27,28], were detected in the 34–46 eV range. These species carry large amounts of kinetic energy [28].

Though an NH_3 double ionization energy of 45.5±0.5 eV has been measured by PIPICO [10], the first differentiated ionization efficiency curve of NH_3^{2+} does not show any structure between 40 and 66 eV [13]. A broad maximum observed between 43 and 55 eV could be indicative of autoionization events at the expense of highly excited NH_3^+ states.

4.2. The NH^+ dissociation channel

The lowest appearance energy measured for NH^+ is at 16.9±0.1 eV, in fairly good agreement with the latest reported value of 17.2 eV [2]. This process, of low intensity, is represented by only one point in fig. 9, i.e. no translational energy is carried away by NH^+ at this threshold.

From the data listed in table 1, the lowest onset for the production of NH^+ from NH_3 corresponding to

$$NH_3 + e^- \rightarrow NH^+(X\,^2\Pi) + H_2(X\,^1\Sigma_g^+) + 2e^-, \quad (1)$$

is calculated at 17.43±0.2 eV. As already pointed out for NH_2^+, a systematic discrepancy is observed between the predicted and measured appearance energies, i.e. 0.5±0.3 eV. This difference contains both the uncertainty on $D(NH_2–H)$ as well as on $D(NH–H)$. In the case of NH_2^+ this difference was 0.24±0.13 eV. Both the results on NH_2^+ and NH^+ support an overestimate of the dissociation energies listed in table 1, for $D(NH_2–H)$ at least.

A second onset of NH^+, corresponding to a more steeply rising portion in the first differentiated ionization efficiency curve (see fig. 8), is observed at 18.0±0.2 eV. This appearance energy has probably to be compared with the early determination of Mann et al. [1] at 19.4±0.5 eV. In this work the onset at 18.0 eV is observed over a retarding potential range of 150 mV (see vertical line (1) in fig. 9). The narrowness of this range together with the independence of this threshold on the retarding field are interpreted by the production of NH^+ without translational energy. The energy difference of $18.0-16.9=1.1\pm0.3$ eV is too low to be ascribed to the electronic excitation of NH^+ into its $A\,^2\Sigma^-$ state. This energy separation is 2.674 eV, as determined by optical spectroscopy (see table 1). Therefore the excess energy of about 1 eV has very likely to be ascribed to

the production of vibrationally excited $NH^+(X\,^2\Pi)$ ions.

The combination of $^2\Pi$ and $^1\Sigma_g^+$ spectroscopic terms in the C_{3v} symmetry would give rise to a ^2E molecular state, i.e. the symmetry of the NH_3^+ first excited state. The photoelectron band corresponding to this state shows a broadening of vibrational structure which is smeared out on the high-energy side [21]. The same state is known to be split into two components by Jahn–Teller distortion, e.g. $^2A' + {}^2A''$ in the C_s symmetry group [9]. As shown by quantum mechanical calculations, the conical intersection between the $\tilde{X}\,^2A''$ and $\tilde{A}\,^2A''$ leads to the NH_2^+ formation at 15.72 eV [9]. The other component of the Jahn–Teller split ^2E could converge to the dissociation limit observed at and above 16.9 eV. Though its band shape suggests that the ^2E state converges to a higher dissociation limit, i.e. above 18.5 eV, Jahn–Teller distortion could lead the $NH_3^+(\tilde{A}\,^2A')$ state to dissociate at 16.9 eV through vibrational predissociation.

At 22.6 ± 0.2 eV, the first differentiated ionization efficiency curve of NH^+ shows a very steep increase. This observation is in good agreement with that of Morrison and Traeger [2] who observed a significant increase at 23.0 eV. Märk et al. [3] measured the lowest onset for NH^+ at 22.9 ± 0.5 eV and Mann et al. [1] determined the second threshold energy of NH^+ at 23.7 ± 0.5 eV.

The dependence of this onset on the ion translational energy, given by diagram (2) in fig. 9, is characterized by (i) a straight line extrapolating to 21.6 eV with a slope of 0.11 and a correlation coefficient of the least-squares fit of 0.999 and (ii) a vertical tail at about 26.5 eV.

When the excess energy with respect to the dissociation limit is entirely converted into kinetic energy of the fragments, the expected slope of the straight line (2) is given by the ratio $2/17 = 0.117$, in close agreement with the measured slope. The energy gap of $22.6 - 16.9 = 5.7$ eV is large enough to involve excitation energy of NH^+ or dissociation energy of H_2 and/or translational energy of the fragments. The two most probable processes at the energy of 22.6 eV would be

$$NH_3 + e^- \rightarrow NH_3^{**}$$
$$\rightarrow NH^+(X\,^2\Pi) + 2H + 2e^-;$$
$$\rightarrow NH^+(C\,^2\Sigma^+) + H_2(X\,^1\Sigma_g^+) + 2e^-,$$

for which a thermodynamical threshold (see table 1) is calculated at 21.90 and 21.84 eV respectively. On the basis of the first onset at 16.9 eV, the onsets for the same reactions are calculated at 21.4 and 21.3 eV. In both cases, there is good agreement between the predicted and the extrapolated value of 21.6 eV. The difference between the observed and the extrapolated onsets, i.e. $22.6 - 21.6 = 1.0$ eV, has only to be ascribed to the total translational energy carried by the fragments, i.e. $0.1 \times 17/2 = 0.85$ eV. The kinetic energy of the NH^+ ions is distributed between 0.1 and 0.5 eV, i.e. 0.85–4.25 eV in terms of total translational energy. Consequently, there is no argument to favour the one or the other reaction. Even more, both processes could take place. Reed and Snedden [4] proposed the former interpretation for their 26.1 eV onset. Mann et al. [1] ascribed their threshold of 23.7 eV to the same dissociation scheme.

The dissociative ionization process giving rise to NH^+ at 22.6 eV occurs where no direct ionization cross section is measured in the photoelectron spectrum of NH_3. It has once more to be pointed out that the NH_2^+ ion has an onset at the same energy. In a similar way, the production of NH^+ at 22.6 eV has to be ascribed to dissociative autoionization. The neutral NH_3^{**} state, involved in both dissociative ionization processes, is probably a Rydberg state member of a series converging to the $NH_3^+(\tilde{B}\,^2A_1)$ state at 24.0 eV.

The vertical tail observed at 26.5 eV (see diagram (2) in fig. 9) lies in the energy range of the $NH_3^+(\tilde{B}\,^2A_1)$ state. The photoelectron band corresponding to this state looks essentially structureless and is likely unstable in the Franck–Condon region. At this energy NH^+ ions carry at least 0.8 eV translational energy or 6.8 eV in terms of total kinetic energy. A rough energy balance calculation would locate the zero-kinetic energy onset at $(AE)_{KE=0} \leqslant 20$ eV which could be correlated with the dissociation

$$NH_3 + e^- \rightarrow NH_3^+(\tilde{B}\,^2A_1)$$
$$\rightarrow NH^+(A\,^2\Sigma^-/B\,^2\Delta) + H_2(X\,^1\Sigma_g^+) + 2e^-,$$

for which the onset is predicted at 20.1/20.3 eV or 16.9+2.7/2.9=19.6/19.8 eV.

A change of slope in the first differentiated ionization efficiency curve is observed at 24.4±0.3 eV. This onset is in good agreement with the value of 24.6 eV published by Morrison and Traeger [2]. The onset of 23.7±0.5 eV, determined by Mann et al. [1] is very probably an average of two energies at 22.6 and 24.4 eV. The threshold measured at 27.2±0.5 eV by Märk et al. [3] disagrees with all these measurements.

The dependence of this appearance energy upon the retarding potential is given by diagram (3) in fig. 9. The linear portion extrapolates to 23.6 eV with a slope of 0.12. A vertical tail is observed at 28.8 eV for $0.7 < V_R < 1.0$ V.

To account for the energy difference of about 2.0±0.6 eV between the two extrapolated values, only internal energy of NH^+ could be invoked, i.e. either vibrational or electronic excitation. The $NH^+(A\,^2\Sigma^-)$ state lies at 2.67 eV above its ground state and the onset calculated for

$$NH_3 + e^- \rightarrow NH_3^+(\hat{B}\,^2A_1)$$
$$\rightarrow NH^+(A\,^2\Sigma^-) + 2H(^2S_g) + 2e^-$$

is at 24.57±0.2 eV using the data listed in table 1, and 24.0 eV starting from the first onset at 16.9 eV.

On the other hand, for 1 eV translational energy, the $(AE)_{KE=0}$ onset of NH^+ can be estimated to be 28.8−8.5=20.5 eV. This value is about the same as obtained for the ions produced at 26.5 eV. Therefore the same dissociation scheme has to be involved.

The NH_3^+ state operative in these reactions has to be the $\tilde{B}\,^2A_1$ state whose adiabatic ionization energy is about 24.0 eV and extends to 30 eV.

Two appearance energies are measured in the double ionization energy range, i.e. 36.2±0.3 and 46.5±0.5 eV. The kinetic energy versus appearance energy diagrams related to these thresholds are shown in fig. 10. Even when in principle single ionization could account for the NH^+ ion production at these energies, no data are available to argue. On the other hand, the analysis of H^+ and H_2^+ ion formation in the same energy range, strongly favours double ionization processes [26].

Energetically, the lowest dissociation process leading to NH^+ is

$$NH_3 + e^- \rightarrow NH_3^{2+}$$
$$\rightarrow NH^+(X\,^2\Pi) + H_2^+(X\,^2\Sigma_g^+) + 3e^-$$

and would require 32.8 eV, as calculated using the data listed in table 1, or 32.3 eV referring to the onset at 16.9 eV determined in this work. The measured energy exceeds the calculated onset by 36.2−32.8(32.3)=3.4(3.9) eV. The threshold at 32.6 eV is observed up to 0.4 eV kinetic energy, i.e. 3.4 eV total translational energy (see fig. 10). For H_2^+ an onset is measured at 35.6±0.3 eV. This critical energy is observed up to 3.4 eV kinetic energy, i.e. 3.8 eV in terms of total energy [26]. These measurements are confirmed by the analysis of D_2^+ formation from ND_3 [26].

The good correlation of these measurements allows us to assign the abovementioned dissociation process to the critical energy at 36.2 eV. However, the accuracy does not allow us to find out whether the $^1A_1$ or the ^3E state of NH_3^{2+} is involved.

To the appearance energy at 46.4±0.5 eV correspond NH^+ ions carrying 0.9 eV translational energy (see fig. 10). Whereas no H_2^+ ions are detected in this energy range, protons are observed at 45.7±0.4 eV. Very likely the dissociation of a doubly ionized state would produce both ions at the same energy.

The threshold energy calculated for the dissociation process

$$NH_3 + e^- \rightarrow NH_3^{2+}$$
$$\rightarrow NH^+(X\,^2\Pi) + H^+ + H(^2S_g) + 3e^-$$

lies at 35.5 eV, using the data listed in table 1. To account for the experimental onset energy, the total translational energy of 17/2×0.9=7.6 eV has to be added and the appearance energy for NH^+ production in its ground vibronic state would require 43.1 eV. The difference between this energy and the observed onset is about 3 eV. The formation of NH^+ in an electronic excited state, e.g. the $A\,^2\Sigma^-$ or $B\,^2\Delta$ state, is probable.

By PIPICO experiments a threshold is measured at 44.5±0.5 eV for coincidences between H^+ and NH^+ or N^+ [10]. Very likely this observation is related to the dissociative ionization process discussed above.

5. Conclusions

The recording of the translational energy distribution for increasing electron energy and the measurement of the appearance energies at different retarding potential settings, enabled a detailed discussion of the formation of both ND_2^+ (NH_2^+) and NH^+ ions in ammonia.

At the lowest threshold energy of these fragment ions, the predissociation of the Jahn–Teller split $NH_3^+(\tilde{A}\,^2E)$ produces ND_2^+ (NH_2^+) and NH^+ as well. The present measurements, together with photoionization and photoelectron spectroscopic data on the NH_2 and NH radicals, tend to show an overestimate of at least the NH_2–H dissociation energy.

In the 20–40 eV electron energy range, and more particularly at 26.6 eV, dissociative autoionization produces both ions. Obviously an NH_3^* Rydberg state, member of a series converging to $NH_3^+(\tilde{B}\,^2A_1)$ is concerned. This neutral state plays an important role in all dissociation channels of NH_3^+.

In the 35–50 eV electron energy range mainly direct dissociation of doubly ionized states of NH_3 is involved. Arguments are brought forward from measurements on (i) ionization energies of NH_3^+, (ii) appearance energies of ND_2^+ (NH_2^+) and NH^+ and of D^+ (H^+) and D_2^+ (H_2^+) observed from ND_3 (NH_3).

Acknowledgement

We acknowledge the Fonds de la Recherche Fondamentale Collective (FRFC), the Université de Liège and the Action de Recherches Concertées (ARC) of the Belgian Government for financial support. One of us (ML) is indebted to the Belgian Government for a PREST grant.

References

[1] M.M. Mann, A. Hustrulid and J.T. Tate, Phys. Rev. 58 (1940) 340.
[2] J.D. Morrison and J.C. Traeger, Intern. J. Mass Spectrom. Ion Phys. 11 (1973) 277.
[3] T.D. Märk, F. Egger and M. Cheret, J. Chem. Phys. 67 (1977) 3795.
[4] R.I. Reed and W. Snedden, J. Chem. Soc. (1959) 4132.
[5] V.H. Dibeler, J.A. Walker and H.M. Rosenstock, J. Res. Natl. Bur. Stand. 70 A (1966) 459.
[6] K.E. McCulloh, Intern. J. Mass Spectrom. Ion Phys. 21 (1976) 333.
[7] G. Sahlstrom and I. Szabo, Arkiv Fysik 38 (1968) 145.
[8] E. von Puttkamer, Z. Naturforsch. 25a (1970) 1062.
[9] C. Krier, M. Th. Praet and J.C. Lorquet, J. Chem. Phys. 82 (1985) 4073.
[10] D. Winkoun and G. Dujardin, Z. Physik D 4 (1986) 57.
[11] G.R. Wight, M.J. van der Wiel and C.E. Brion, J. Phys. B 10 (1977) 1863.
[12] C.E. Brion, A. Hamnett, G.R. Wight and M.J. van der Wiel, J. Electron Spectry. 12 (1977) 323.
[13] R. Locht and J. Momigny, Chem. Phys. Letters 138 (1987) 391.
[14] R. Locht and J. Schopman, Intern. J. Mass Spectrom. Ion Phys. 15 (1974) 361.
[15] Ch. Servais, R. Locht and J. Momigny, Intern. J. Mass Spectrom. Ion Processes 71 (1986) 179.
[16] C.E. Moore, Atomic energy levels, Vol. 1, NBS Circular 467 (Natl. Bur. Std, Washington, 1949).
[17] B. de B. Darwent, Bond dissociation energies in simple molecules, NSRDS-NBS 31 (1970).
[18] G. Herzberg, Molecular spectra and molecular structure, Vol. 2 (Van Nostrand, Princeton, 1950).
[19] S.J. Dunlavey, J.M. Dyke, N. Jonathan and A. Morris, Mol. Phys. 39 (1980) 1121.
[20] R. Colin and A.E. Douglas, Can. J. Phys. 46 (1968) 61.
[21] J.W. Rabalais, L. Karlsson, L.O. Werme, T. Bergmark and K. Siegbahn, J. Chem. Phys. 58 (1973) 3370.
[22] A.W. Potts, T.A. Williams and W.C. Price, Faraday Discussions Chem. Soc. 54 (1972) 104.
[23] G. Bieri, L. Åsbrink and W. von Niessen, J. Electron Spectry. 27 (1982) 129.
[24] R. Camilloni, G. Stefani and A. Giardini-Guidoni, Chem. Phys. Letters 50 (1973) 213.
[25] F. Tarantelli, A. Tarantelli, A. Sgamellotti, J. Schirmer and L.S. Cederbaum, Chem. Phys. Letters 117 (1985) 577.
[26] R. Locht, Ch. Servais, M. Ligot and J. Momigny, to be published.
[27] J. Kurawaki and T. Ogawa, Chem. Phys. 86 (1984) 295.
[28] B.L. Carnahan, W.W. Kao and E.C. Zipf, J. Chem. Phys. 74 (1981) 5149.